

# Analyses of winter circulation types and their impacts on haze pollution in Beijing

He Jianjun<sup>1\*</sup>, Gong Sunling<sup>1</sup>, Zhou Chunhong<sup>1</sup>, Lu Shuhua<sup>1</sup>, Wu Lin<sup>2\*</sup>, Chen Ying<sup>3</sup>, Yu Ye<sup>4</sup>, Zhao Suping<sup>4</sup>, Yu Lijuan<sup>5</sup>, , ChengmeiYin<sup>5</sup>

<sup>1</sup>State Key Laboratory of Severe Weather & Key Laboratory of Atmospheric Chemistry of CMA, Chinese Academy of Meteorological Sciences, Beijing 100081, China

<sup>2</sup>The College of Environmental Science & Engineering, Nankai University, Tianjin 300071, China

<sup>3</sup>Lancaster Environment Centre, Lancaster University, Lancaster, LA1 4YQ, UK

<sup>4</sup>Northwest Institute of Eco-Environment and Resources, Chinese Academy of Sciences, Lanzhou 730000, China

<sup>5</sup>Jinan Meteorological Bureau, Jinan 250002, China

11

\*Correspondence to: He Jianjun ([hejianjun@camsma.cn](mailto:hejianjun@camsma.cn)) and Wu Lin ([envwu@vip.qq.com](mailto:envwu@vip.qq.com))

13

Abstract: For a better understand the interannual variation of winter haze pollution, this study classifies winter circulation types and investigates their impacts on local meteorology and haze pollution from 1980 to 2017 in Beijing. Circulation types are classified by T-mode principal component analysis combined with the K-means cluster method using European Centre for Medium-range Weather Forecasts ERA-interim sea level pressure data. The results can effectively distinguish the cold air-mass processes, degeneration of cold air-mass, and stagnant weather conditions. Usually, cold air-mass process over Beijing is accompanied by a low temperature, high relative humidity, large pressure gradient and near-surface wind speed, and deep mixing layer. The cold air-mass process facilitates pollutants dispersion and transport them outside Beijing, and hence lower PM<sub>2.5</sub> concentration and frequencies of haze events. In contrast, the local meteorology and haze pollution were almost the inverse for stagnant weather. The local meteorological conditions and haze pollution for the degeneration of cold air are between the previous circulation types. Based on PM<sub>2.5</sub> observation during 2010-2017, the occurrence frequency of cold air was low in the recent winters of 2013, 2014 and 2017, and resulted in severe PM<sub>2.5</sub> pollution. High frequency of stagnant weather (48.4%) was one of the reasons that haze pollution reached 37% during 1980-2017 over Beijing. The time series of haze frequency was negatively correlated with that of cold air frequency. During 38

30 winters from 1980 to 2017, a decreased trend of haze days was found, which was partly related to an  
31 increased trend of cold air frequency. However, the trends of haze days and cold air in Beijing were  
32 not significant based on regression analysis.

33  
34 Keywords: circulation types, local meteorology, haze pollution, PM<sub>2.5</sub>

## 35 **1. Introduction**

36 Haze is defined as large amounts of inactivated fine particles floating in the atmosphere that result  
37 in low visibility (less than 10 km) and turbid air. It is a weather phenomenon and a natural weather  
38 disaster (Zhang et al., 2013). With rapid economic development, haze pollution has occurred  
39 frequently and has attracted attention from governments, the public, and researchers. Severe haze,  
40 which is mainly caused by serious aerosol pollution, is not a completely natural phenomenon in China  
41 (Zhang et al., 2013). And it also affects meteorological processes, such as precipitation (Guo et al.,  
42 2016). The formation of haze decreases atmospheric visibility, affects the production and daily live,  
43 and has an adverse impact on human health (An et al., 2015). Unfortunately, at least 30% of the area  
44 and nearby 800 million people in China are affected by different degrees of haze (Che et al., 2009).  
45 There were relatively few annual haze days in the 1960s, but they increased sharply in the 1970s,  
46 remained stable to 1995, and then increased from 1995 to 2012 in North China Plain (Chen et al.,  
47 2015). Understanding the formation mechanisms of haze is very important for haze prevention.

48 Pollutant emission and meteorological conditions are two key factors for haze pollution, and high  
49 pollutant emission is the primary cause. According to the China Statistical Yearbook, the emission of  
50 sulfur dioxide, nitric oxide and dust reached  $1.86 \times 10^7$ ,  $1.85 \times 10^7$ , and  $1.54 \times 10^7$  tons, respectively, in  
51 2015 (<http://www.stats.gov.cn/tjsj/ndsj/2016/indexch.htm>). Meteorological condition is another  
52 important factor for haze pollution. Meteorological parameters, such as temperature, relative humidity,  
53 wind speed, and boundary layer height, are significantly correlated with pollutant concentrations in  
54 most Chinese cities and explained more than 70% of the variance of daily average pollutant  
55 concentrations (He et al., 2017a). In January 2013, a persistent severe haze event occurred over  
56 eastern China. Unusual meteorological conditions were responsible for this persistent severe haze  
57 event (Zhang et al., 2014). The long term trend of haze is regional and seasonal dependent. Haze  
58 showed decreasing trends during 30 winters from 1981 to 2010, while summertime haze displayed

59 continuous increasing trends, and obvious regional difference of haze trends was detected in southern  
60 Hebei province (Fu et al., 2014). The weakening of near-surface winds during 1985-2005 caused the  
61 increase in winter haze days over eastern China (Yang et al., 2016). At different spatial scales,  
62 meteorological conditions can be divided into a large-scale circulation type and local meteorological  
63 conditions. The circulation type governs local meteorological conditions and is effective in the  
64 identification of haze pollution (Oanh et al., 2005); it is the main factor driving the day-to-day  
65 variations in pollutant concentrations (Lee et al., 2012). Although many studies have investigated the  
66 relation between circulation type and haze pollution (or air quality) (Demuzere et al., 2009; He et al.,  
67 2016a; He et al., 2017a; Jiang et al., 2014; Jiang et al., 2016; Lee et al., 2012; Oanh et al., 2005;  
68 Pearce et al., 2011; Zhang et al., 2012), this relation can also vary with time, location and pollutants  
69 (Jiang et al., 2017).

70 Beijing, as the capital of China, has frequently suffered severe haze pollution in winter. Many  
71 pollutant emission sources surround Beijing, and local vehicle emissions, special terrain and  
72 meteorological conditions are the main reasons for haze pollution in Beijing (He et al., 2016b).  
73 Horizontal transport of pollutants, which is affected by atmospheric circulation, may be the most  
74 important factor determining the air quality of Beijing (Miao et al., 2017). Some studies have focused  
75 on the relation between circulation types and air pollution in Beijing and the surrounding region (Chen  
76 et al., 2008; Chen et al., 2009; Li et al., 2012; Meng and Cheng, 2002; Miao et al., 2017; Zhang et al.,  
77 2012). However, few studies have analysed the long-term winter circulation types by using an  
78 objective method and investigated their relationships with haze pollution in Beijing and surrounding  
79 regions. This article extends our previous work (He et al., 2017b) by using long-term data to  
80 investigate the thermal and dynamical characteristics of circulation types and their impacts on local  
81 meteorological conditions and haze pollution over Beijing. Because haze pollution is most severe in  
82 winter, this paper focuses on the winter circulation type. This result can help us understand the  
83 development of haze events and is useful for haze forecasting and prevention over Beijing and similar  
84 areas.

## 85 **2. Data and method**

### 86 **2.1 Meteorological data**

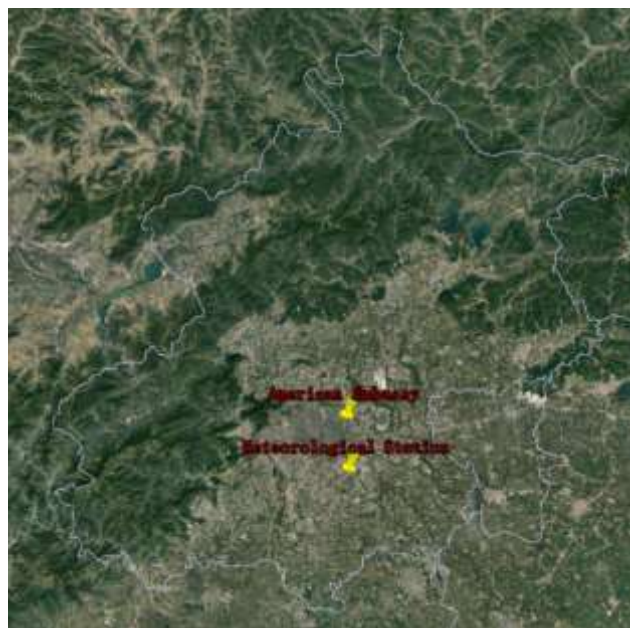
87 The European Centre for Medium-range Weather Forecasts (ECMWF) ERA-interim reanalysis

88 data (<https://www.ecmwf.int/en/research/climate-reanalysis/era-interim>) for 38 winters (December to  
89 February) from 1980 to 2017 were used in this study. The spatial and temporal resolutions of ECMWF  
90 ERA-interim data are 0.25° and 6 hours (i.e., 08:00, 14:00, 20:00, 02:00 local standard time every  
91 day), respectively. Sea Level Pressure (SLP) for the area of 110°E-125°E/35°N-45°N was used to  
92 identify circulation type following previous studies (He et al., 2017b; Jiang et al., 2017; Zhang et al.,  
93 2012). Temperature and dew point temperature at 850 hPa, 700 hPa, and 500 hPa from the ECMWF  
94 ERA-interim reanalysis data were used to calculate the K index, which represents atmospheric  
95 thermal unstable capacity in the middle-low troposphere (Zhang et al., 2014). The equation for the K  
96 index is given in following:

$$97 \quad K = (T_{850} - T_{500}) + T_{d850} - (T_{700} - T_{d700}) \quad (1)$$

98 where K is the K index and  $T_{850}$ ,  $T_{700}$ , and  $T_{500}$  are temperatures at 850 hPa, 700 hPa, and 500  
99 hPa, respectively.  $T_{d850}$  and  $T_{d700}$  are the dew point temperatures at 850 hPa and 700 hPa,  
100 respectively. According to the definition of the K index, a larger K index represents a more unstable  
101 middle-low tropospheric atmosphere.

102 Near-surface daily climatological data (including daily average temperature, relative humidity,  
103 wind speed and wind direction) during 38 winters from 1980 to 2017 at Beijing station were acquired  
104 from the National Meteorological Information Center (<http://data.cma.cn/site/index.html>). These  
105 datasets were used to construct a relation between circulation type and local meteorological  
106 conditions. The location of Beijing station is shown in Figure 1.



107  
108 Figure 1. The location of air quality monitoring stations (American Embassy) and meteorological

109 station.

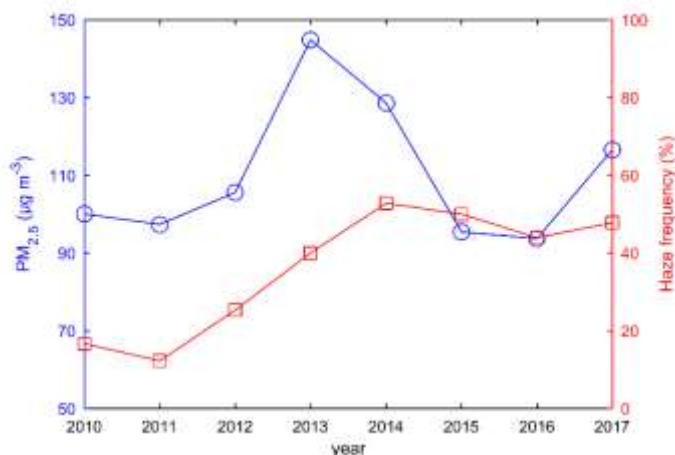
## 110 **2.2 Air quality data**

111 Haze is mainly caused by aerosol pollution (Zhang et al., 2013). A new ‘Ambient air quality  
112 standard’ was published in 2012 by the Ministry of Environmental Protection and the General  
113 Administration of Quality Supervision, Inspection and Quarantine of China. Particulate matter with  
114 aerodynamic diameter less than 2.5  $\mu\text{m}$  ( $\text{PM}_{2.5}$ ) was introduced in the air quality index system for the  
115 first time in China. However, long-term continuous observation of  $\text{PM}_{2.5}$  is few in China.  $\text{PM}_{2.5}$   
116 concentration was observed and released (<http://www.stateair.net/web/post/1/1.html>) since 2008 in  
117 American Embassy in Beijing (Figure 1). The monitoring station represents urban-traffic type in  
118 Beijing. Considering data integrity,  $\text{PM}_{2.5}$  concentrations in American Embassy during 8 winters from  
119 2010 to 2017 were used to analyze the impact of circulation type on aerosol concentration. The data  
120 quality control method for  $\text{PM}_{2.5}$  concentration is described in our previous study (He et al., 2017a).

## 121 **2.3 Haze days**

122 With an increase in humidity, hygroscopic growth occurs on fine particles, which then activate as  
123 cloud condensation nuclei and finally convert haze to fog. Visibility, particulate matter and relative  
124 humidity are thus three important properties of haze. Because of the absence of long-term particulate  
125 matter observation, only days with visibility less than 10 km and relative humidity less than 90% are  
126 defined as haze days based on previous studies (Yang et al., 2016). Based on visibility and relative  
127 humidity, winter haze days from 1980 to 2017 at Beijing station were obtained from the National  
128 Meteorological Information Centre.

129 Aerosol scattering and absorption of visible light deteriorate atmospheric visibility. Haze pollution  
130 is closely related to the loading of aerosol. Time series of average  $\text{PM}_{2.5}$  concentration and occurrence  
131 frequency of haze days are shown in Figure 2. Relatively low  $\text{PM}_{2.5}$  concentration accompany with a  
132 high occurrence frequency of haze is observed in 2015 and 2016. The possible reason maybe the  
133 change of relative humidity or chemical components of  $\text{PM}_{2.5}$  which affects optical characteristics of  
134 aerosol.



135

136 Figure 2. Time series of average PM<sub>2.5</sub> concentration and occurrence frequency of haze days during  
 137 8 winters from 2010 to 2017.

### 138 2.4 Circulation types

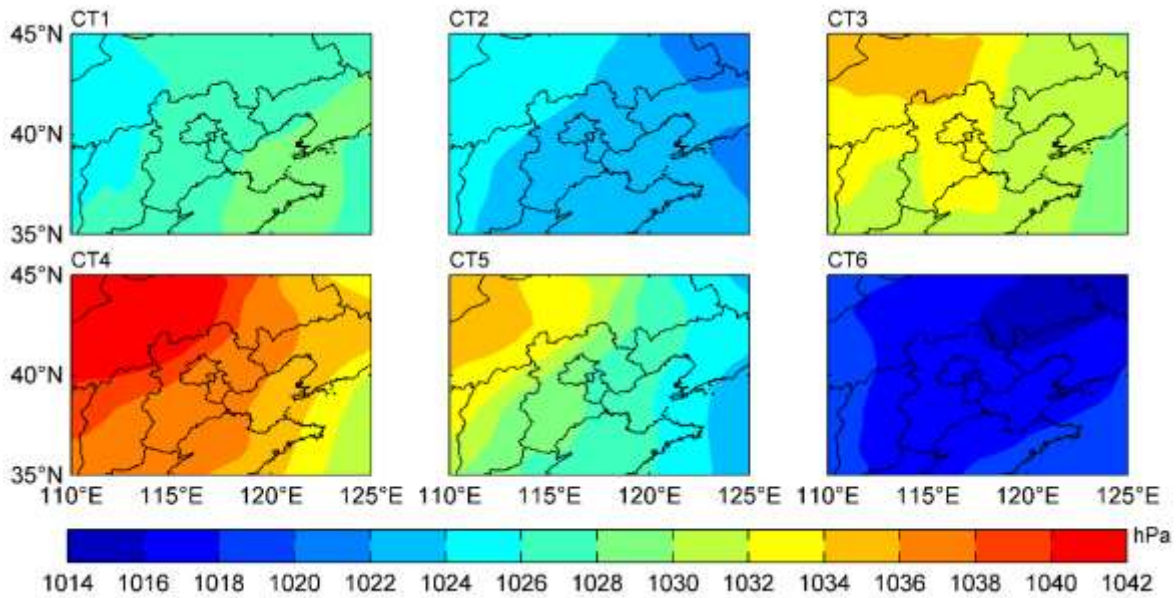
139 Five main circulation classification techniques, namely the correlation method, cluster analysis,  
 140 principal component analysis (PCA), the fuzzy method, and nonlinear methods, have been frequently  
 141 used to classify circulation types (Zhang et al., 2012). In this study, T-mode PCA combined with K-  
 142 means cluster is used, because previous researchers have proposed this is the best approach for  
 143 revealing data structures and effectively identifying circulation types (Huth, 1996). And this method  
 144 has been widely used in previous studies in China (He et al., 2016a; He et al., 2017a; He et al., 2017b;  
 145 Miao et al., 2017; Zhang et al., 2012). Data processing to determine circulation type included five  
 146 steps. First, three-dimensional ERA SLP grid data (longitude × latitude × time) was reshaped to two-  
 147 dimensional data (grid × time). Second, data was normalized using z-scores method. Third, the  
 148 normalized data performed PCA. Fourth, main components were acquired according to the  
 149 cumulative variance contribution of 85%. Fifth, the main components were clustered using the K-  
 150 means cluster, and synoptic-scale circulations were ascertained based on cluster results. The number  
 151 of clusters depends on the criterion function (Liu and Gao, 2011), and the inflection of the criterion  
 152 function represents the optimal number of clusters. Finally, six circulation types were determined (i.e.,  
 153 CT1 to CT6). The weather and diffusion characteristics of six circulations are discussed in the  
 154 following.

### 155 **3. Results and Discussion**

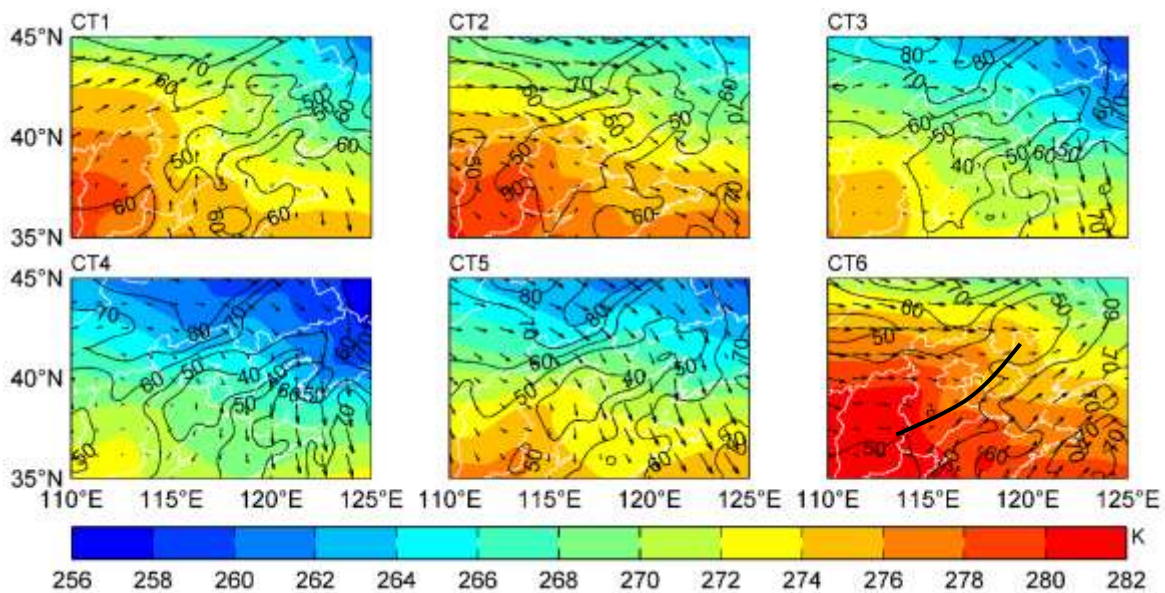
#### 156 **3.1 Circulation types and weather characteristics**

157 Winter climate characteristics in North China are closely related to the winter monsoon. Previous  
158 studies have revealed that a strong winter monsoon is beneficial to pollutant dispersion over Beijing  
159 and surrounding regions (Liu et al., 2017). The change of winter circulation types is a direct indicator  
160 of winter monsoon intensity. Using the T-mode PCA combined with the K-means cluster, six  
161 circulation types are identified. The meteorological fields at each moment are assigned to one  
162 circulation type. The mean meteorological fields for six circulation types are calculated. Figure 3  
163 shows the mean SLP of six circulation types. According to the spatial distribution of SLP, CT4 showed  
164 the strongest cold air synoptic process in North China, with a cold high pressure that reached 1040  
165 hPa and covered Inner Mongolia. Figure 4 shows the spatial distribution of meteorological fields for  
166 six circulation types at 1000 hPa. Most parts of North China were controlled by north winds for CT4.  
167 The bottom of high pressure formed an obvious anti-cyclone. A southwest-northeast dry belt was  
168 located in the centre of North China and the temperature gradient was large. Low temperature, low  
169 relative humidity, and high wind speed were typical weather characteristics over Beijing for the CT4  
170 circulation type. The cold air synoptic process of CT5 was weaker than that of CT4. Compared with  
171 CT4, similar weather characteristics for CT5 were found in North China (Figure 3). CT3 was a  
172 degeneration of cold air in North China. The pressure gradient of CT3 was significantly smaller than  
173 that of CT4 and CT5. Although the meteorological pattern was similar to that of CT4 and CT5, the  
174 wind speed (temperature) decreased (increased) remarkably over Beijing. With small pressure  
175 gradients, CT1, CT2 and CT6 are typical stagnant weather. For CT1, Beijing was in the rear of a weak  
176 high-pressure system. Most parts of North China were controlled by southern and southwestern wind.  
177 The temperature and humidity in Beijing and surrounding regions were affected by warm advection  
178 and water vapour transport were relatively high. For CT2, weak northwest wind covered most parts  
179 of North China. Wind decreases significantly from northwest to southeast of North China. Spatial  
180 distribution of wind was unfavourable for the ventilation capacity over Beijing. For CT6, a weak low-  
181 pressure system existed in Northeast China, and the pressure gradient was very weak in North China.  
182 Affected by surface pressure, the northwest region of Beijing was covered by western wind, whereas  
183 the southeast region to Beijing was covered by southwest wind. The change of the wind field formed

184 a convergence zone. Atmospheric block resulted in low wind speed over Beijing. Temperatures were  
 185 high over Beijing because of warm advection (Figure 4). Based on characteristics of meteorological  
 186 fields over Beijing and surrounding areas, CT4 and CT5 can be defined as the cold air process, CT3  
 187 is defined as weak or degenerate cold air, CT1, CT2 and CT6 are defined as stagnant weather.



188  
 189 Figure 3. Mean sea level pressure of six circulation types during 38 winters from 1980 to 2017.



190  
 191 Figure 4. Mean temperature (shade), relative humidity (contour line), and wind field (arrow) of six  
 192 circulation types at 1000 hPa during 38 winters from 1980 to 2017. Black lines represent convergence  
 193 lines.

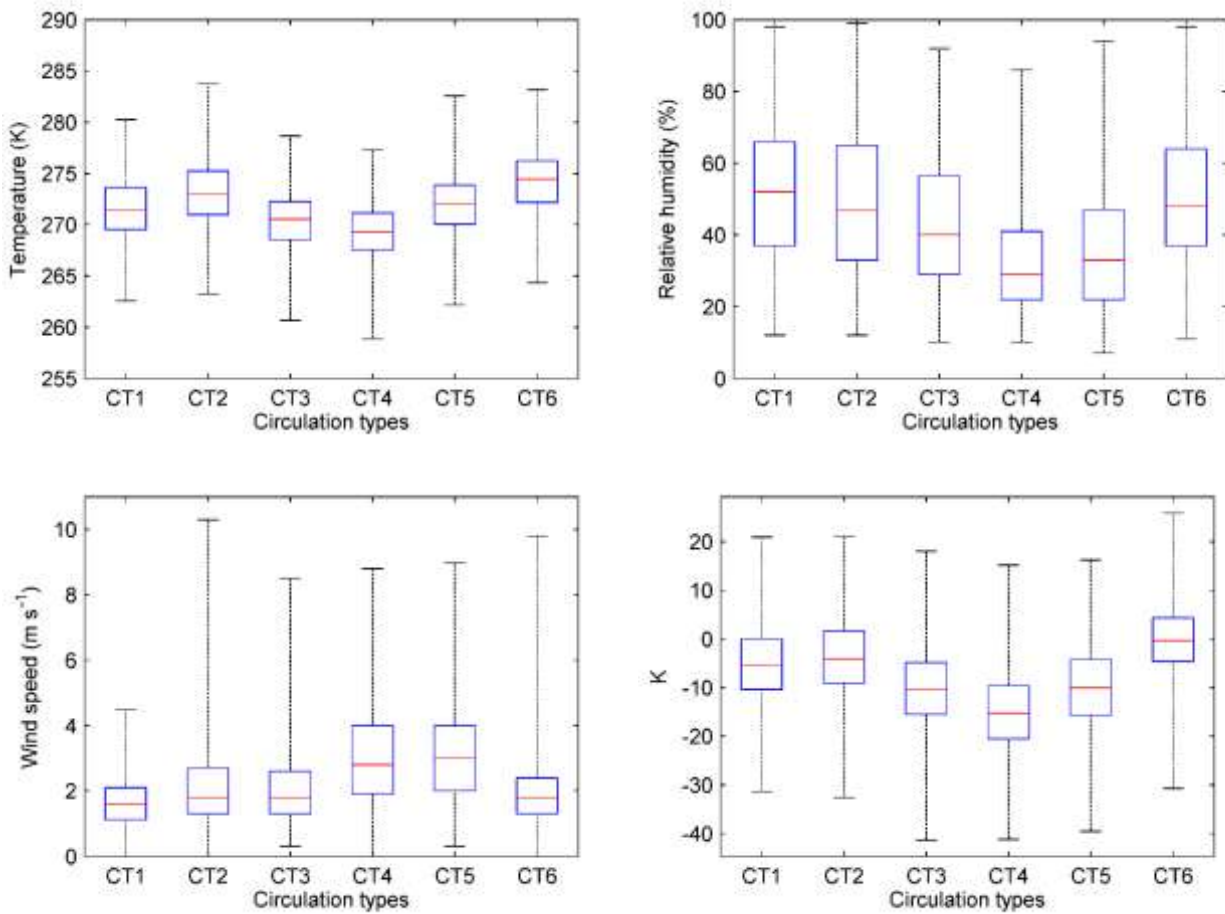
194 Based on statistical analysis, the occurrence frequencies for CT1 to CT6 were 16.5%, 19.1%,



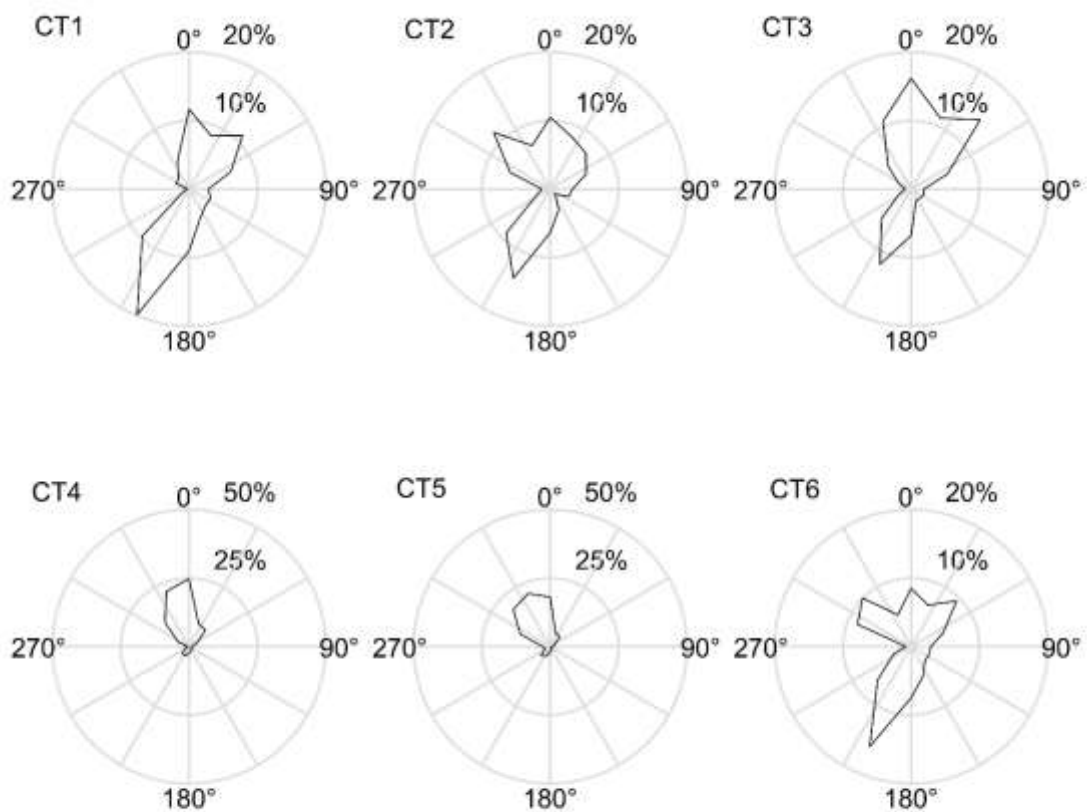
195 20.7%, 14.3%, 16.6%, and 12.8%, respectively. The occurrence frequency of stagnant weather (CT1,  
196 CT2 and CT6) reached 48.4%, and 30.9% for the cold air process (CT4 and CT5), which is conducive  
197 to ventilation. The cold air process often occurred in night and morning (02:00 and 08:00, Beijing  
198 Time). The evolution of circulation types is an important issue, and there is an evolution between the  
199 cold air process and stagnant weather in North China. When cold air breaks out, the circulation type  
200 is CT4 or CT5. With the movement of cold air from the northwest to the southeast, cold air  
201 degenerates and the circulation type becomes CT3, followed by CT1, and CT2. After a period of cold  
202 air accumulation over Siberia and Outer Mongolia, a new cold air process breaks out, and the  
203 circulation type changes from CT2 to CT4 or CT5. Another evolution between CT2 and CT6 was  
204 found.

205 Local meteorological conditions were closely related to synoptic scale circulation types and  
206 underlying surface condition. Figure 5 shows the box graph of surface meteorological parameters at  
207 the Beijing meteorological station (Figure 1) for six circulation types during 38 winters from 1980 to  
208 2017. To be consistent with daily average surface meteorological parameters, a circulation type for  
209 one day is defined as a type that appears twice a day or more at four times (08:00, 14:00, 20:00, and  
210 02:00) a day. Circulation types governed local surface meteorological parameters, and meteorological  
211 parameters had significant differences for different circulation types based on variance analysis at the  
212 95% confidence level. The source of cold high pressure was in Outer Mongolia and Siberia. The cold  
213 air process brought a significant decrease of temperature and humidity over Beijing. According to  
214 geostrophic wind theory, wind speed is positively correlated with the pressure gradient. The cold air  
215 process resulted in a large pressure gradient and brought large winds over Beijing. The predominant  
216 direction in surface was north and northwest wind for CT4 and CT5 respectively (Figure 6). Winter  
217 cold high pressure in East Asia is a relatively shallow weather system, and the average thickness of  
218 cold high pressure is no more than 3 km. The cold air process decreased low level temperature and  
219 the K index and resulted in stable atmospheric stratification in the middle-low troposphere (upper  
220 boundary layer). For stagnant weather, the local meteorological parameters were contrary to those for  
221 the cold air process, i.e., 2-m temperature, 2-m relative humidity and K index were large, whereas the  
222 10-m wind speed was small in Beijing. The predominant direction in surface was southwest wind  
223 (Figure 6). Northwest wind was a second prevailing wind for CT2 and CT6. It is interesting that  
224 atmospheric stratification in the middle-low troposphere was more stable for the cold air process than

225 for stagnant weather based on the comparison of the K index. For degeneration of cold air, the local  
226 meteorological parameters were between the cold air and stagnant weather. North, northeast, and  
227 southwest wind were the main wind direction in surface for CT3 (Figure 6).



229  
230 Figure 5. Box graph of surface pressure (a), 2-m temperature (b), 2-m relative humidity (c) and 10-m  
231 wind speed (d) in Beijing for six circulation types during 38 winters from 1980 to 2017.

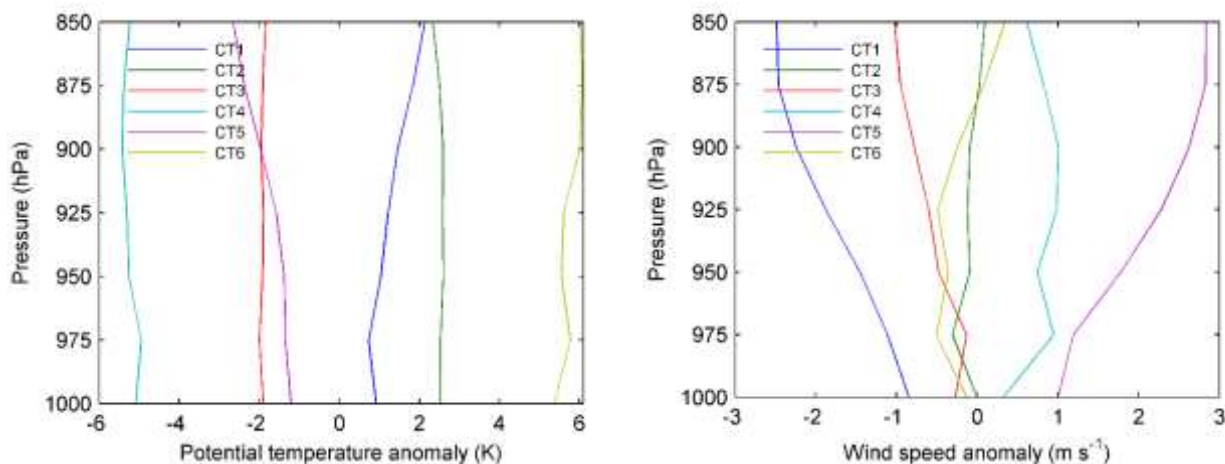


232

233 Figure 6. Wind rose map in Beijing for six circulation types during 38 winters from 1980 to 2017.

234 Boundary layer structures are also governed by atmospheric circulation (Miao et al., 2017). Figure  
 235 7 shows vertical profiles of potential temperature and wind speed anomaly for six circulation types.  
 236 A cold bias of potential temperature was detected for CT4 and CT5. Cold bias increased with height  
 237 for CT4 and CT5, which implies that the cold air process increased the atmospheric temperature lapse  
 238 rate and turbulent mixing in the boundary layer by a thermal process and formed a deep mixing layer.  
 239 A positive bias of wind speed was detected for CT4 and CT5, and the positive bias increased with  
 240 height in the boundary layer. This characteristic of vertical profiles of wind speed anomaly for CT4  
 241 and CT5 resulted in an increase of vertical wind shear and formed a deep mixing layer by dynamical  
 242 processes. For stagnant weather, i.e., CT1, CT2, and CT6, an opposite change of the vertical profiles  
 243 of potential temperature and wind speed anomaly was found and formed a shallow mixing layer by  
 244 thermal and dynamical processes compared with the cold air process (CT4 and CT5). For CT3,  
 245 potential temperature and wind speed were smaller than the average climatological values in the  
 246 boundary layer. The bias of potential temperature was constant at different heights, whereas the

247 negative bias of wind speed increased with height, which restrained the development of turbulence  
248 by dynamical processes. In general, the cold air process (stagnant weather) formed a deep (shallow)  
249 mixing layer by affecting local atmospheric thermal and dynamical processes. These results did not  
250 contradict the K index because of different atmospheric height levels.

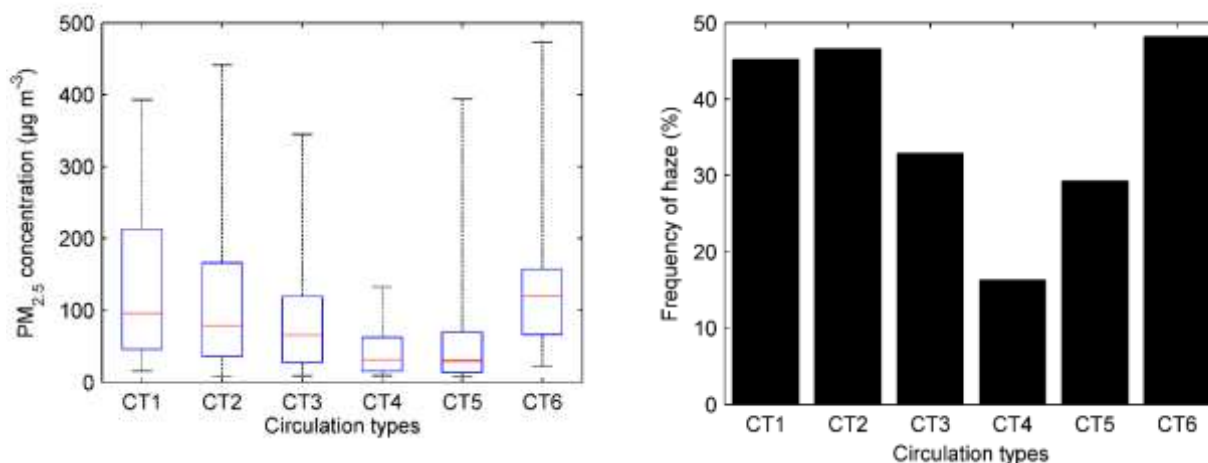


251  
252 Figure 7. Vertical profiles of potential temperature anomaly (a) and wind speed anomaly (b) in Beijing  
253 for six circulation types during 38 winters from 1980 to 2017.

### 254 3.2 Impact of weather type on PM<sub>2.5</sub> and haze pollution

255 Atmospheric circulation had an obvious impact on near-surface PM<sub>2.5</sub> concentration (Figure 8a).  
256 Variance analysis revealed that the different circulation types had significant differences in PM<sub>2.5</sub>  
257 concentration at the 95% confidence level. Previous studies revealed that PM<sub>2.5</sub> concentration was  
258 positively correlated with 2-m temperature and 2-m relative humidity and was negatively correlated  
259 with 10-m wind speed over the North China Plain; the correlation passed the t-test at a 95%  
260 confidence level (He et al., 2017a; He et al., 2017b; Liu et al., 2017). With low temperature, low  
261 relative humidity, and high wind speed, the cold air process (CT4 and CT5) was favourable for  
262 pollutant dispersion and brought low PM<sub>2.5</sub> concentration. After the cold air process (CT3), the  
263 atmospheric dispersion capability weakened, and pollutant accumulation resulted in the increase of  
264 PM<sub>2.5</sub> concentration. Stagnant weather (CT1, CT2 and CT6) was accompanied by high temperature,  
265 high humidity and low wind speed, which was unfavourable for pollutant dispersion. For CT1,  
266 southwestern wind transported pollutants from south of Hebei province (He et al., 2017c; Miao et al.,  
267 2017) and exacerbated atmospheric pollution over Beijing. A convergence near Beijing for CT6  
268 formed pollutant accumulation. Additionally, the atmospheric stratification in the middle-low  
269 troposphere was unstable for stagnant weather (i.e., large K index). Unstable atmospheric

270 stratification favours the formation of cloudy and rainy weather accompanied by high humidity and  
 271 is conducive to aerosol hygroscopic growth (Zhang et al., 2014). The aerosols in the middle-low  
 272 troposphere decreased near-surface shortwave radiation and then restrained turbulence development.  
 273 Mixing layer height is another important factor that affects air pollution (He et al., 2017a). The cold  
 274 air process (stagnant weather) formed a deep (shallow) mixing layer and enhanced (weakened) the  
 275 vertical mixing of pollutants, accompanied by low (high) PM<sub>2.5</sub> concentration.



276  
 277 Figure 8. Box graph of daily mean PM<sub>2.5</sub> concentration (a) during 4 winters from 2010 to 2017 and  
 278 occurrence frequency of haze days (b) during 38 winters from 1980 to 2017 for six circulation types.

279  
 280 Table 1 shows the average PM<sub>2.5</sub> concentration and occurrence frequency of cold air for each winter  
 281 from 2010 to 2017. The Chinese Ambient Air Quality Standards (CAAQS) Grade II standards of  
 282 annual mean PM<sub>2.5</sub> concentration is 35 µg m<sup>-3</sup>. The mean PM<sub>2.5</sub> concentration in 8 winters in Beijing  
 283 is 3.2 times of the Grade II value, which implies severe air pollution due to large amount of pollutant  
 284 emissions. The correlation coefficients between winter average PM<sub>2.5</sub> concentration and occurrence  
 285 frequency of six circulation types and cold air are 0.85, 0.71, 0.14, -0.41, -0.67, -0.37, and -0.65,  
 286 respectively. Based on t-test, the correlation coefficients are significant for CT1, CT2 and CT5 at 95%  
 287 confidence interval. The frequency of cold air was only 25%, 21% and 23% in the winters of 2013,  
 288 2014 and 2017, and a stagnant circulation of CT1 exceeded 20% in winter 2013 and 2017, which was  
 289 adverse for PM<sub>2.5</sub> transport and dispersion to the outside and facilitated the accumulation of pollutants.  
 290 The average PM<sub>2.5</sub> concentration reaches 145 µg m<sup>-3</sup>, 129 µg m<sup>-3</sup>, and 117 µg m<sup>-3</sup> in winter 2013,  
 291 2014 and 2017. Although the frequencies of cold air and stagnant weather in winter 2017 are close to  
 292 that in winter 2013, the PM<sub>2.5</sub> concentration is significant low in winter 2017 due to great emission

293 control measures. The frequency of cold air reached 41% in the winters of 2012 and 2016. Although  
 294 the atmospheric circulation was favourable for pollutant dispersion, the average PM<sub>2.5</sub> concentration  
 295 still reached 106 µg m<sup>-3</sup> and 94 µg m<sup>-3</sup> in the winters of 2012 and 2016, respectively, which indicates  
 296 that air pollution is very serious in Beijing. Large amounts of pollutant emissions are the main reason  
 297 for serious air pollution in the studied area (He et al., 2017a).

298

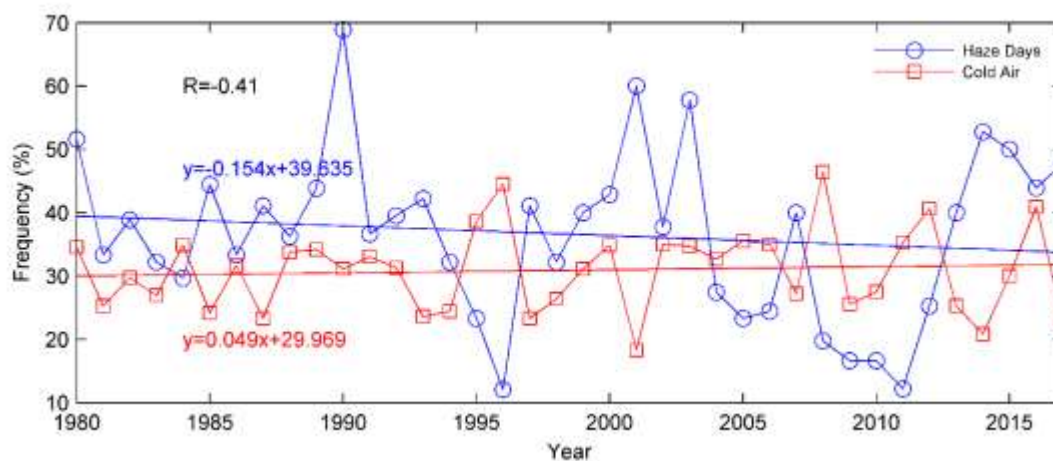
299 Table 1. PM<sub>2.5</sub> concentration (mean and standard deviation, µg m<sup>-3</sup>) and occurrence frequency of  
 300 circulation type (%) for each winter from 2010 to 2017.

	2010	2011	2012	2013	2014	2015	2016	2017
PM <sub>2.5</sub> concentration	100±74	97±103	106±90	145±11	129±10	95±79	94±106	117±10
Frequency of CT1	15	10	12	29	16	14	13	22
Frequency of CT2	18	16	16	20	19	15	16	23
Frequency of CT3	20	13	27	18	27	23	20	25
Frequency of CT4	13	21	22	11	11	9	18	8
Frequency of CT5	15	14	19	14	9	21	23	15
Frequency of cold air	27	35	41	25	21	30	41	23

301

302 Correlated with aerosols and visibility, haze is disastrous weather. Similar to the PM<sub>2.5</sub> analysed  
 303 above, haze pollution is closely affected by atmospheric circulation (Fig. 6b). A low frequency of  
 304 haze days was found under cold air processes (i.e., CT4 and CT5), and a high frequency was found

305 for stagnant weather. Figure 9 shows time series of frequency of haze days and cold air. The average  
 306 occurrence frequency of haze days for the 38 winters was 37%, with a maximum value of 69% (1990)  
 307 and a minimum value of 12% (1996). The correlation coefficient between the time series of frequency  
 308 of haze days and cold air frequency during the 38 winters reached -0.41 ( $p < 0.1$ ), which implies that  
 309 the interannual variation of haze days was closely related to the interannual variation of cold air. In  
 310 some extreme winters, such as those in 1996, 2008, and 2012, strong cold air improved air quality  
 311 and decreased the frequency of haze days. Linear regression analysis revealed that frequency of  
 312 winter haze decreased from 1980 to 2017, whereas the frequency of cold air slightly increased. The  
 313 decreased trend of haze may have been partly caused by the increased trend of cold air. However, the  
 314 trend of interannual variation of winter haze and cold air was not significant at the 95% confidence  
 315 level. Artificial measurement of atmospheric visibility has been progressively replaced by automatic  
 316 measurement since 2011. The bias between artificial measurement and automatic measurement of  
 317 atmospheric visibility has introduced some uncertainty for haze pollution. Yang et al. (2016)  
 318 investigated winter haze over eastern China from 1980 to 2014 and found that haze days increased  
 319 from 21 days in 1980 to 42 days in 2014. The annual haze increased from 1995 to 2012 in North  
 320 China (Chen et al., 2015). The trend of haze days in this paper is different from those in Yang et al.  
 321 (2016) and Chen et al. (2015), partly because of the different study areas and seasons considered.  
 322 Significant regional difference of the trends of haze days was also detected in Hebei province (Fu et  
 323 al., 2014). And the trends of haze pollution was different from nearby Hebei province, which implies  
 324 that haze pollution and interannual trends have obvious local characteristics due to local meteorology  
 325 and local emissions.



326  
 327 Figure 9. Time series of occurrence frequency of haze days and cold air during 38 winters from 1980

328 to 2017. The blue and red lines represent the liner regression trend for haze days and cold air,  
329 respectively.

#### 330 **4. Conclusion**

331 Pollutant emissions and meteorological conditions are two key factors that determine haze  
332 pollution. Synoptic scale atmospheric circulation governs local meteorological values and the  
333 boundary layer and thus affects local air quality. Using observations of PM<sub>2.5</sub> concentrations, haze  
334 days based on visibility and relative humidity, meteorological observations and reanalysis data, this  
335 paper investigated winter atmospheric circulation types, and their relationship with local  
336 meteorological conditions and haze pollution over Beijing.

337 Six circulation types were identified that could significantly distinguish the cold air process (a  
338 degeneration of cold air) and stagnant weather. The evolution of atmospheric circulation is also  
339 analysed. For the cold air process, a large pressure gradient was found in North China with cold high  
340 pressure located over northwest of North China, accompanied by low temperature, high relative  
341 humidity, and large winds over Beijing. Temperatures and wind speed anomalies for cold air in the  
342 boundary layer implied that strong turbulence triggered by thermal and dynamical processes formed  
343 a deep mixing layer. However, the analysis of the K index revealed that stable atmospheric  
344 stratification in the middle-low troposphere (the upper boundary layer) was detected for the cold air  
345 process. Cold air facilitated pollutant dispersion and transport to the outside, and then lower PM<sub>2.5</sub>  
346 concentration and frequency of haze days. The pressure gradient was very small in North China for  
347 stagnant weather, resulting in a calm weather condition with relatively high temperature, low relative  
348 humidity, low near-surface wind speed, and shallow mixing layer depth. Based on an analysis of the  
349 K index, atmospheric stratification was unstable in the middle-low troposphere (the upper boundary  
350 layer) compared with the cold air process. A convergence line was found surrounding Beijing surface  
351 layer, and southerly winds brought pollutants from Hebei province. Stagnant weather was adverse for  
352 pollutant dispersion and transport and facilitated the accumulation of pollution in Beijing. For the  
353 degeneration of cold air, the local meteorological conditions and haze pollution were between those  
354 of previous circulation types.

355 The interannual variations of PM<sub>2.5</sub> concentration and haze days were significantly affected by the  
356 variation of atmospheric circulation. PM<sub>2.5</sub> observations revealed that PM<sub>2.5</sub> pollution was severe in



357 the winters of 2013, 2014 and 2017, which was caused by low frequency of cold air and high  
358 frequency of stagnant weather. The average occurrence frequency of haze days for the 38 winters  
359 reached 37%. The high frequency of stagnant weather (48.4%) was one of the reason for the haze  
360 pollution. The frequency of haze days was negatively correlated with the frequency of cold air, with  
361 a correlation coefficient of -0.41 ( $p < 0.1$ ). Vice versa, a decreased trend of haze days during winter  
362 from 1980 to 2017 was partly related to an increased trend of cold air frequency. However, these  
363 trends were not significant based on regression analysis.

364

365 **Acknowledgements:** This work was supported by the National Natural Science Foundation of China  
366 (No. 41705080 and 91544232), CAMS Basis Research Project (No. 2017Y001), the National Science  
367 and Technology Infrastructure Programme (No. 2014BAC16B03), and the CMA Innovation Team  
368 for Haze-fog Observation and Forecasts.

369

## 370 **Reference:**

371 An, X.Q., Tao Y., Mi, S.Q., Sun, Z.B., Hou Q., 2015. Association between PM<sub>10</sub> and Respiratory  
372 Hospital Admissions in Different Seasons in Lanzhou. *J. Environ. Health*, 77, 64-71.

373 Che, H.Z., Zhang, X.Y., Li, Y., Zhou, Z.J., Qu, J.J., Hao, X.J., 2009. Haze trends over the capital cities  
374 of 31 provinces in China, 1981-2005. *Theoretical and Applied Climatology*, 97, 235-242, doi:  
375 10.1007/s00704-008-0059-8.

376 Chen, Z.H., Cheng, S.Y., Li, J.B., Guo, X.R., Wang, W.H., Chen, D.S., 2008. Relationship between  
377 atmospheric pollution processes and synoptic pressure patterns in northern China. *Atmos.*  
378 *Environ.*, 42, 6078-6087, doi:10.1016/j.atmosenv.2008.03.043.

379 Chen, Y., Zhao, C. S., Zhang, Q., Deng, Z. Z., Huang, M. Y., and Ma, X. C., 2009. Aircraft study of  
380 Mountain Chimney Effect of Beijing, China. *J. Geophys. Res.*, 114, D08306,  
381 doi:10.1029/2008JD010610.

382 Chen, H.P., Wang, H.J., 2015. Haze Days in North China and the associated atmospheric circulations  
383 based on daily visibility data from 1960 to 2012. *J. Geophys. Res. Atmos.*, 120, 5895-5909, doi:  
384 10.1002/2015JD023225.

385 Demuzere, M., Trigo, R.M., Vila-Guerau de Arellano, J., van Lipzig, N.P.M., 2009. The impact of

386 weather and atmospheric circulation on O<sub>3</sub> and PM<sub>10</sub> levels at a rural mid-latitude site. *Atmos.*  
387 *Chem. Phys.*, 9, 2695-2714.

388 Fu, G.Q., Xu, W.Y., Yang, R.F., Li, J.B., Zhao, C.S., 2014. The distribution and trends of fog and haze  
389 in the North China Plain over the past 30 years. *Atmos. Chem. Phys.*, 14, 11949-11958.  
390 doi:10.5194/acp-14-11949-2014.

391 Guo, J., Deng, M., Lee, S.S., Wang, F., Li, Z., Zhai, P., Liu, H., Lv, W., Yao, W., Li X., 2016. Delaying  
392 precipitation and lightning by air pollution over the Pearl River Delta. Part I: Observational  
393 analyses, *J. Geophys. Res. Atmos.*, 121, 6472-6488, doi:10.1002/2015JD023257.

394 He, J.J., Yu, Y., Xie, Y.C., Mao, H.J., Wu, L., Liu, N., Zhao, S.P., 2016a. Numerical model-based  
395 artificial neural network model and its application for quantifying impact factors of urban air  
396 quality. *Water Air Soil Pollut.*, 227, 235, doi: 10.1007/s11270-016-2930-z.

397 He, J.J., Wu, L., Mao, H.J., Liu, H.L., Jing, B.Y., Yu, Y., Ren, P.P., Feng, C., Liu, X.H., 2016b.  
398 Development of a vehicle emission inventory with high temporal-spatial resolution based on  
399 NRT traffic data and its impact on air pollution in Beijing-Part 2: Impact of vehicle emission on  
400 urban air quality. *Atmos. Chem. Phys.*, 16, 3171-3184, doi:10.5194/acp-16-3171-2016.

401 He, J.J., Gong, S.L., Yu, Y., Yu, L.J., Wu, L., Mao, H.J., Song, C.B., Zhao, S.P., Liu, H.L., Li, X.Y.,  
402 Li, R.P., 2017a. Air pollution characteristics and their relationship to meteorological conditions  
403 during 2014-2015 in Chinese major cities. *Environ. Pollut.*, 223, 484-496, doi:  
404 10.1016/j.envpol.2017.01.050.

405 He, J.J., Gong, S.L., Liu, H.L., An, X.Q., Yu, Y., Zhao, S.P., Wu, L., Song, C.B., Zhou, C.H., Wang,  
406 J., Yin, C.M., Yu, L.J., 2017b. Influence of meteorological conditions on interannual variations  
407 of particle matter pollution during winter the Beijing-Tianjin-Hebei area. *Journal of*  
408 *Meteorological Research*, 31, 1062-1069, doi:10.1007/s13351-017-7039-9.

409 He, J.J., Mao, H.J., Gong, S.L., Yu, Y., Wu, L., Liu, H.L., Chen, Y., Jing, B.Y., Ren, P.P., Zou, C.,  
410 2017c. Investigation of particulate matter regional transport in Beijing based on numerical  
411 simulation. *Aerosol and Air Quality Research*, 17, 1181-1189, doi:10.4209/aaqr.2016.03.0110.

412 Huth, R., 1996. An intercomparison of computer-assisted circulations classification methods. *Int. J.*  
413 *Climatol.*, 16, 893-922.

414 Jiang, N.B., Dirks, K.N., Luo, K., 2014. Effects of local, synoptic and large-scale climate conditions  
415 on daily nitrogen dioxide concentrations in Auckland, New Zealand. *Int. J. Climatol.*, 34, 1883-

416 1897, doi: 10.1002/joc.3808.

417 Jiang, N.B., Scorgie, Y., Hart, M., Riley, M.L., Crawford, J., Beggs, P.J., Edwards, G.C., Chang, L.,  
418 Salter, D., Virgilio, G.D., 2017. Visualising the relationships between synoptic circulation type  
419 and air quality in Sydney, a subtropical coastal-basin environment. *Int. J. Climatol.*, 37,1211-  
420 1228, doi: 10.1002/joc.4770.

421 Lee, C.C., Ballinger, T.J., Domino, N.A., 2012. Utilizing map pattern classification and surface  
422 weather typing to relate climate to the air quality index in Cleveland, Ohio. *Atmos Environ*, 63,  
423 50-59, doi: 10.1016/j.atmosenv.2012.09.024.

424 Li, L.J., Wang, Y., Li, J.X., Xin, L.Z., Jin, J., 2012. The analysis of heavy air pollution in Beijing  
425 during 2000-2010. *China Environmental Science*, 32, 23-30 (in Chinese).

426 Liu, D., Gao, S.C., 2011. Determining the number of clusters in K-means clustering algorithm. *Silicon*  
427 *Valley*, 6, 38-39 (in Chinese).

428 Liu, T.T., Gong, S.L., He, J.J., Yu, M., Wang, Q.F., Li, H.R., Liu, W., Zhang, J., Li, L., Wang, X.G.,  
429 Li, S.L., Lu, Y.L., Du, H.T., Wang, Y.Q., Zhou, C.H., Liu, H.L., Zhao, Q.C., 2017. Attributions  
430 of meteorological and emission factors to the 2015 winter severe haze pollution episodes in  
431 China's Jing-Jin-Ji area. *Atmos. Chem. Phys.*, 17, 2971-2980, doi:10.5194/acp-17-2971-2017.

432 Meng, Y.J., Cheng, C.L., 2002. Impact of surface synoptic situations on air pollution in Beijing area.  
433 *Meteorological Monthly*, 28, 42-47 (in Chinese).

434 Miao, Y.C., Guo, J.P., Liu, S.H., Liu, H., Li, Z.Q., Zhang, W.C., Zhai, P.M., 2017. Classification of  
435 summertime synoptic patterns in Beijing and their associations with boundary layer structure  
436 affecting aerosol pollution. *Atmos. Chem. Phys.*, 17, 3097-3110, doi:10.5194/acp-17-3097-2017.

437 Oanh, N.T.K., Chutimon, P., Ekbordin, W., Supat, W., 2005. Meteorological pattern classification and  
438 application for forecasting air pollution episode potential in a mountain-valley area. *Atmos*  
439 *Environ*, 39, 1211-1225, doi: 10.1016/j.atmosenv.2004.10.015.

440 Pearce, J.L., Beringer, J., Nicholls, N., Hyndman, R.J., Uotila, P., Tapper, N.J., 2011. Investigating  
441 the influence of synoptic-scale meteorology on air quality using self-organizing maps and  
442 generalized additive modelling. *Atmos. Environ.*, 45, 128-136, doi:  
443 10.1016/j.atmosenv.2010.09.032.

444 Yang, Y., Liao, H., Lou, S.J., 2016. Increase in winter haze over eastern China in recent decades Roles  
445 of variations in meteorological parameters and anthropogenic emissions. *J. Geophys. Res.*

446 Atmos., 121, 13050-13065, doi: 10.1002/2016JD025136.

447 Zhang, J.P., Zhu, T., Zhang, Q.H., Li, C.C., Shu, H.L., Ying, Y., Dai, Z.P., Wang, X., Liu, X.Y., Liang,  
448 A.M., Shen, H.X., Yi, B.Q., 2012. The impact of circulation patterns on regional transport  
449 pathways and air quality over Beijing and its surroundings. *Atmos. Chem. Phys.*, 12, 5031-5053,  
450 doi: 10.5194/acp-12-5031-2012.

451 Zhang, R.H., Li, Q., Zhang, R.N., 2014. Meteorological conditions for the persistent severe fog and  
452 haze event over eastern China in January. *Science China: Earth Sciences*, 57, 26–35, doi:  
453 10.1007/s11430-013-4774-3.

454 Zhang, X.Y., Sun, J.Y., Wang, Y.Q., Li, W.J., Zhang, Q., Wang, W.G., Quan, J.N., Cao, G.L., Wang,  
455 J.Z., Yang, Y.Q., Zhang, Y.M., 2013. Factors contributing to haze and fog in China. *Chin Sci*  
456 *Bull*, 58, 1178-1187, doi: 10.1360/972013-150 (in Chinese).